Egypt. J. Bot., **Vol. 62,** No.3, pp. 687-707 (2022)

Egyptian Journal of Botany
http://ejbo.journals.ekb.eg/

Effect of Biologically and Chemically Synthesized AgNPs on Multi-Drug Resistant (MDR) Dermatophyte Bacterial Isolates

Gehan A. Ismail, Nanis G. Allam, Reda M. Gaafar, Marwa M. El Zanaty[#], Perihan S. Ateya
Department of Botany, Faculty of Science, Tanta University, Tanta 31527, Egypt.

IN THIS study, silver nanoparticles (AgNPs) were synthesized using biological and chemical methods. Trisodium citrate (TSC) was used as a reducing and stabilizing agent in the chemical method. While three seaweed aqueous extracts from *Enteromorpha intestinalis*, *Sargassum vulgare*, and *Asparagopsis taxiformis* and two cyanobacteria filtrates from *Spirulina platensis*, and *Oscillatoria acuminata* were utilized in the biological method. The production of the synthesized AgNPs was verified through UV-Vis spectroscopy analysis. Both of the synthesized AgNPs exhibited remarkable antibacterial activity against multidrug-resistant pathogenic bacterial isolates of *Staphylococcus aureus* (S1), *Escherichia coli* (E1), *Klebsiella pneumoniae* (K1), *Staphylococcus epidermidis* (S5), and *Pseudomonas auroginosa* (P1) when compared with sulfamethoxazole as the control. AgNPs biologically synthesized using *S. vulgare* aqueous extract exhibited the maximum antibacterial activity and were further characterized by X-ray diffraction (XRD) diffraction, Fourier transform infrared spectroscopy analysis (FTIR), and transmission electron microscopy (TEM). XRD revealed crystalline shape of AgNPs with a mean size of 28.93 and 29.31 nm for the chemically and biologically synthesized AgNPs, respectively; and Zeta potential was recorded at −50.3±10.4 and −52.1±10.8 mV, respectively. Moreover, the AgNPs (100 µg/mL) were safe for human fibroblast normal cell lines at 24h. Both types of AgNPs were loaded onto polylactic acid/ polyethylene glycol (PLA/PEG) films, and a significant antibacterial activity was observed against S1 and E1 after 3 and 6h of treatment. Thus, these results demonstrate the potential use of biologically synthesized AgNPs from seaweeds for wound infection treatments and therapeutic applications as a safe and economic alternative to chemical agents.

Keywords: Cyanobacteria, Cytotoxicity, Infection treatments, PLA/PEG/ Ag-NPs nanofilms, Seaweeds, Wound healing.

Introduction

Nanotechnology is a flourishing research field focusing on the strategic synthesis, and handling of particles measuring 1–100nm in size (Wang & Herron, 1991). Recently, nanoparticles (NPs) have been widely used in multiple fields such as health care, food, and environmental health (Khan et al., 2019). Among the various types of metallic nanoparticles, silver nanoparticles (AgNPs) have been specifically studied for their unique physical, chemical, and natural properties. AgNPs have been used successfully in several fields, including pharmaceutics, agriculture, water purification, food industry and as catalytic agents in oxidation reactions (Gupta et al., 2017; Aslam et al., 2021). Due to their broad-spectrum antimicrobial potential, AgNPs are known to have strong bactericidal effects against various bacterial species and are extremely toxic to gram-negative and gram-positive microorganisms, including multidrug-resistant (MDR) bacteria (Loo et al., 2018; Abdelmawgoud et al., 2022). Furthermore, they are inexpensive and induce, low cytotoxicity, with minimum immunological response when applied in *in vivo* studies (Samuel et al., 2020).

[#]Corresponding author email: marwa_51338_pg@science.tanta.edu.eg Tel. 01003569753
Received 27/02/2022; Accepted 21/05/2022
DOI: 10.21608/ejbo.2022.120076.1905
Edited by: Prof. Dr. Wael N. Hozzein, Faculty of Science, Beni-Suef University, Egypt.

Bacteria are the causative agents of several diseases. For instance, *Escherichia coli* causes urinary tract infection, diarrhea, and meningitis. *Pseudomonas aeruginosa* thrives on medical instruments such as ventilators and catheters, and often causes nosocomial infection (Zazo et al., 2016). Similarly, *Staphylococcus aureus* is responsible for skin, joint infections, bacteremia, and sepsis. Due to the constantly increasing number of bacterial infections, it has become crucial to discover new antibiotic resources and new strategies to combat bacterial resistance and modifications (Chinnasamy et al., 2021). Chemically developed drugs exhibit several side effects; therefore, the efficiency of metallic nanoparticles, especially AgNPs, in tackling infectious syndromes is emerging as an exciting solution with varied applications (Lee et al., 2019). Moreover, there has been a growing interest in synthesizing new nanomaterials using various biological agents resulting in advancement of the field. Marine macroalgae (seaweeds) is one of the commercially vital renewable living resources (Bhuyar et al., 2020; Menaa et al., 2021). The biological synthesis of AgNPs using seaweeds is a simple, clean, viable, and cost-effective green technology (Zhang et al., 2020). These NPs are protected with different types of biomolecules, such as proteins and polysaccharides present in the seaweed, which can enhance their stability and enhance their biological activity (Ballotin et al., 2016). In this regard, several studies have indicated that AgNPs stimulate wound healing and demonstrate antimicrobial properties against a broad range of wound invading dermatophyte bacteria, including *P. aeruginosa*, *E. coli,* and *S. aureus* (Othman et al., 2019; Stan et al., 2021). Wound dressings containing chemically synthesized AgNPs have also been recommended to enhance wound healing by reducing the inflammatory response of wound cells (Krishnan et al., 2020; Nqakala et al., 2021). Therefore, incorporating biosynthesized AgNPs into a composite film of polylactic acid and polyethylene glycol (PLA/PEG) could improve the free radical scavenging capacity and antibacterial properties of a nanomaterial against dermatophyte strains (Turalija et al., 2016; Mahmoudi et al., 2019).

In this study, AgNPs were synthesized using seaweed and cyanobacteria using biological method and compared with those synthesized using chemical method. The antibacterial effect of these nanoparticles was investigated against wound-invading bacterial pathogens. Additionally, the application of these biological AgNPs either alone or in combination with PLA/PEG films as wound bandages was investigated.

Materials and Methods

Identification and isolation of bacterial isolates

Bacterial isolates were generally obtained from Microbiology laboratory, Faculty of Pharmacy, Tanta University, Egypt. The isolates were cultured on diverse selective media such as nutrient agar, MacConkey agar, EMB (Eosin methylene blue) agar, as well as cetrimide and mannitol salt agar. Bacterial isolated were purified by sub-culturing, and then the biochemical and morphological inspections were directed repeatedly using the standard microbiological methods as described by Oxoid (1981) and Collee et al. (1996) until complete purification and identification of these bacterial isolates was established.

Investigation of the antibiotic sensitivity of the bacterial isolates

The sensitivity of pathogenic bacterial isolates was evaluated to 13 types of standard antibiotics that belongs to 7 different antimicrobial classes (Bioanalyse, Turkey). These antibiotics were including: amoxicillin–clavulanic acid (AMC), Meropenem (MEM), Cefepime (FEB), Cefuroxime (CXM), Cefotriaxone (CRO), Trimethoprime-Sulfamethoxazole (SXT), Levofloxacin (LEV), Azithromycin (AZM), Aztreonam (AZ), Oxacillin (OXA), Chloramphenicol (CL), Tetracycline (TE), and Streptomycin (S). The experiment was conducted using the disc diffusion method (Kirby-Bauer et al., 1966), and the diameter of the inhibition zones (mm) was measured and assessed according to the Clinical and Laboratory Standards Institute (CLSI, 2021) manual. Furthermore, the multi-antibiotic resistant (MAR) index was specified for each individual isolate by devising the number of antibiotics to which the isolate was resistant by the total number of the tested antibiotics (Vasquez & Hand, 2004). Finally, the most MDR bacterial isolates (which were resistant to at least one antibiotic drug belonging to three or more antibiotic categories (Magiorakos et al., 2014) were further authentically identified using the Biomerieux VITEK® 2 system.

Chemical synthesis of AgNPs

AgNPs were synthesized by using the chemical reduction method (Fang et al., 2005). Fifty ml of silver nitrate ($AgNO_3$) solution (1×10^{-3} M) was heated to boiling. Then, 5mL of 1% trisodium citrate (TSC; $C_6H_5Na_3O_7$), as a reducing and stabilizing agent, were added drop by drop, while stirring. The solution was mixed vigorously during this process and heated until the change of color to pale brown was noticed. At this point, the heating was stopped and the suspension of AgNPs was left to cool at room temperature.

Biological synthesis of AgNPs

Preparation of seaweed extracts

Three types of seaweed from different divisions were collected in 2019 by the Phycological Laboratory members, Faculty of Science, Tanta University from the submerged rocks at low tide along, Alexandria (Abu Qir-Bay) beaches (E 30°03'; N 31°19') and Marsa-Matrouh City (N 31°21'; E 27°14'), Mediterranean coast, Egypt. Seaweed samples were cleaned using tap water followed by distilled water. A portion of the fresh samples were preserved for taxonomical identification. Seaweed samples were identified according to Aleem (1993) and Guiry & Guiry (2019) as: *Enteromorpha intestinalis* (Linnaeus) (Chlorophyta), *Sargassum vulgare* C. Agardh (Phaeophyta), and *Asparagopsis taxiformis* (Delile) (Rhodophyta). The moisture content was removed completely by shading-dried the seaweed samples for 2 weeks (El-Shouny et al., 2017). After that, the seaweed samples were oven-dehydrated at 50°C for 30 min, grounded into powder using a mixer grinder, and finally, stored in an air-tight container at 4°C until used for NPs synthesis.

Preparation of cyanobacteria extract

Axenic cultures of *Spirulina platensis* (Gomont) and *Oscillatoria acuminata* (Gomont) were attained from the Phycological Laboratory, Faculty of Science, Tanta University. The two species were cultured in Zarrouk's medium (Zarrouk, 1966) and BG-11 (Blue-Green algae) medium (Rippka et al., 1979), respectively. The cultures were incubated at 3000 lux of light intensity, air mix of dry air (97%) and CO_2 gas (3%), temperature of 30±2°C, light/dark cycles of 16/8h, and with manual shaking of the cultures thrice a day. The growth was monitored spectrophotometrically at 750nm every 2 days for 21 days. Biomass was collected, washed with distilled water (for 3 repeated times) and centrifuged at 3000rpm for 10min (Ismail et al., 2021a). The pellet was oven dried at 50ºC for 3 days until it reached a constant weight, and the dried powder was stored in closed vials at 4ºC until used for NPs synthesis.

Biosynthesis of AgNPs

Seaweed or cyanobacteria powder weighing 1g was mixed with 100 ml of distilled H_2O in a 250mL Erlenmeyer flask and placed in a water bath at 80°C for 20min. The extract was filtered using a Whatman No. 1 filter paper, followed up by a 0.2µm Millipore filter, and the recovered filtrate was maintained as a stock in a refrigerator at 4ºC (Rajeshkumar et al., 2014). For the preparation of AgNPs, a 10mL of seaweed and/or cyanobacteria aqueous extract was added to 90mL of aqueous $AgNO_3$ (0.001M), and the mixture was gradually heated to 60°C (Suriya et al., 2012). The color change from yellowish to a uniform dark brown was considered as a visible verification of the bio-reduction of $AgNO_3$ to AgNPs. The AgNPs were recovered by centrifugation at 10 000rpm at 30°C for 30 min. The AgNPs residue was oven-dehydrated at 50°C for 5h, pressed into powder and stored in an air-tight container until further investigation (Paul & Yadav, 2014; Ismail et al. 2021b).

Confirmation of AgNPs synthesis by UV-Visible spectroscopy

UV–Vis spectroscopy analysis was performed to confirm the reduction of silver ions (Ag^+) by the chemical and biological extracts. 3mL of the synthesized AgNPs sample was analyzed in a quartz cuvette. The absorbance of the developed color was measured at 300-800 nm on a Shimadzu dual-beam spectrophotometer (model UV 1650 PC) (Chung et al., 2016).

Antibacterial activity test of the synthesized AgNPs

Antibacterial efficacies of the chemically and biologically synthesized AgNPs were evaluated using the agar well diffusion technique against selected MDR bacterial isolates (El-Shouny et al., 2017). Approximately 50µL of either chemically or biologically synthesized AgNPs water suspensions, as well as an $AgNO_3$ solution (negative control), were independently added to the wells of agar plates, as previously described in the above section. The plates were incubated

at 37°C for 18:24h to ensure the formation of a clear growth inhibition zone around the wells. The antibacterial activities of the investigated AgNPs were estimated by measuring the diameter (mm) of the inhibitory zone as previously described (CLSI, 2021). Results were compared with Sulfamethoxazole (SXT) as a standard positive control antibiotic. All the procedures were repeated in triplicate. The most active biologically synthesized AgNPs with maximum antibacterial activity were further characterized.

Characterization of the chemically and biologically synthesized AgNPs

Fourier transform infrared (FTIR) spectroscopy analysis

FTIR analysis was conducted using the potassium bromide pellet technique (Saranya devi et al., 2014), to detect the functional groups in the extracts that might be accountable for the reduction of the silver ions to form AgNPs. The spectrum was assayed in the range of 500–4000cm^{-1} using FTIR instrument (Genesis Series Nicolet IS-10 F, AKX).

X - ray diffraction (XRD) analysis

The size and crystalline shape of the synthesized AgNPs were determined using an XRD instrument (X-ray diffractometer Philips-X'Pert MPD). The results were measured in zone 20, with a range from 4° to 90° (0.5°/min), and the period constant was 2s. The average particle diameter of the formed AgNPs was estimated from the XRD configuration consistent with the line width of the extreme strength reflection peak, and the size of the NPs was valued using Scherrer's equation (Mehta et al., 2017).

Zeta potential measurement

The net surface charge of the synthesized AgNPs was estimated by Zeta potential analysis using the laser zeta-sizer instrument (Malvern zetaseizer instrumentation Co.). Five ml of AgNPs samples were diluted with double distilled water (50mL) using NaCl (2 $x10^{-2}$ M) as a suspending electrolyte solution (Haider & Mehdi, 2014).

Transmission Electron Microscope (TEM) analysis

TEM was performed to determine the morphology and to approve the size of the synthesized AgNPs using an electron microscope (JEOL, TEM 2100 SX) operated at 200 KV (Aswathy & Philip, 2012). The samples were prepared by placing one drop of the AgNPs sample onto a carbon-coated TEM grid, and the grids were dried at room temperature before the analysis was run (Zawrah & Abd El-Moez, 2011).

Cytotoxicity test of the synthesized AgNPs

The cytotoxicity of the synthesized AgNPs was evaluated using (WI-38) fibroblasts, a human cell line derived from the lung tissues of a 3-month-gestation female fetus. Briefly, 100 ml of the cell line (approximately 5000 viable cells) was added to each well of a 96-well microtiter plate and incubated for 12h in a humidified CO_2 incubator at 37°C to obtain monolayers. Then, the tested chemically or biologically synthesized AgNPs were added to the plate at different concentrations of 100, 125, 250, 500, and 1000µg/mL, followed by incubation for another 24 and 48h. Next the plates were treated with CCK-8 kit (Biotech Beyotime Inst, China). Then, the absorbance was measured at 450 nm by a BioTek ELx800 microtiter plate reader (BioTek Instruments Inc., Winooski, VT, USA), and the cell viability was expressed as percentage. Furthermore, the cytotoxicity curve was plotted and the safe concentration (the concentration of AgNPs that showed no toxicity to the cultured normal human cell line and affected the pathogenic bacteria) of the investigated AgNPs was established.

Preparation of silver-loaded (PLA/PEG/AgNPs) nanofilms with antibacterial activity for wound healing assay

Preparation of polylactic acid/polyethylene glycol (PLA/PEG) film loaded with AgNPs

The flexible PLA/PEG (1:1) film was prepared by implementing the solvent volatilization method (Hassan et al., 2019). At 40°C, equivalent weights of PLA and PEG (500mg) were dissolved in 40mL of dichloromethane, then stirred for 30min until a completely homogeneous, clear, and bubble-free solution was formed. The solution was loaded onto a glass petri dish and dehydrated at room temperature for 24h to form a film (nanosilver unloaded PLA/PEG film), and then the film was placed in a vacuum oven for 24h at 50°C to dehydrate completely. The PLA/PEG nanofilms loaded with AgNPs were prepared similarly, with the addition of 50mg of either of the synthesized AgNPs to the mixture solution. Then, the PLA/PEG/AgNPs mixtures

were thoroughly stirred for 60 min. followed by spreading into a petri dish, and dehydrated as previously described for 24h to form a 5% concentration of nanosilver loaded films, PLA/PEG/AgNPs (Hassan et al., 2019).

Determination of the bactericidal capacity of PLA/PEG/AgNPs nanofilms

The bactericidal ability of the prepared PLA/PEG/AgNPs nanofilms was estimated versus the five selected MDR bacterial strains. First, approximately 5µL of the bacterial suspensions was seeded into a 96-well microtiter plate. Then, 10 µl of sterilized loaded nanofilms, PLA/PEG/AgNPs, (at the predetermined safe concentration) was added to each well. Other wells containing the same volume of sterilized unloaded PLA/PEG nanofilms were used as controls. Then, the plate was incubated at 37°C under shaking conditions at 150rpm. Finally, the absorbance was measured at 610nm after 24h of incubation using a microtiter plate reader device, BioTek ELx800, and the resultant percentage of bacterial growth inhibition was estimated using the following equation (Bardania et al., 2020):

$$\text{Bacterial inhibition (\%)} = (Ic - Is)/Ic \times 100$$

where, Ic and Is are the average absorbance value of the control and sample groups, respectively.

Statistical analysis

All tests were conducted in triplicate, and the results were expressed as mean values with standard deviation. Analysis of variance (ANOVA) was used to consider the significant difference in the antibacterial activities of various algal extracts at the significance level of $P \leq 0.05$. This analysis was conducted using the computer program SPSS 24.0 (2016) for Windows (IBM SPSS Statistics for Windows, Version 24.0., IBM Corp Armonk, NY).

Results

Isolation, purification, and sensitivity test of the pathogenic bacterial isolates

A total of 13 bacterial isolates were morphologically and biochemically characterized and identified as 4 gram-positive isolates of *S. aureus* (S1, S2, S3 and S4) and 1 isolate of *S. epidermidis* (S5). Additionally, eight gram-negative isolates were identified, including four isolates of *E. coli* (E1, E2, E3 and E4), two isolates of *K. pneumoniae* (K1 and K2), and two isolates of *P. aeruginosa* (P1 and P2) as listed in Table 1. Based on the antibiotic susceptibility test, these isolates were found to be resistant to more than two standard antibiotics; hence, they were termed as MDR bacterial isolates. The MAR index indicated that all the investigated isolates possessed extreme high MAR index values ranging from 0.6 to 1.0, indicating a resistance percentage of 61-100%. Among these MDR isolates, *S. aureus* (S1) and *E. coli* (E1) showed the maximum resistance percentage (100%), followed by *K. pneumoniae* isolate (K1), *S. epidermidis* isolate (S5) and *P. aeruginosa* isolate (P1) with a resistance percentage of 92%. However, the antibiotic resistance, ranged from 100% for AZM to 61% for AMC, with a common percentage of 92% estimated for S, CXM, LEV, and CL, as shown in Table 1.

The isolates S1, E1, K1, and P1 were further identified by using the Biomerieux VITEK® 2 system due to their extreme resistance. The results revealed a probability percentage of 98% for *S. aureus* (S1) and *K. pneumoniae* (K1) isolates, whereas a probability percentage of 97% was recorded for *E. coli* (E1) and *P. aeruginosa* (P1) isolates, confirming the biochemical and morphological identification results.

Confirmation of the chemically and biologically synthesized AgNPs by UV-Visible spectroscopy

The UV-Vis absorption spectrum or surface Plasmon resonance (SPR) of silver ions was measured at a wavelength range of 300-800nm. In the case of chemically synthesized AgNPs (Fig. 1a), the nanoparticles were generated in a few minutes and the UV spectrum revealed a well-defined SPR centered at approximately 420nm, which is a characteristic feature for AgNPs development. For biosynthesized AgNPs using seaweed extracts, the SPR was measured every 30min until AgNPs generation. The band center varied according to the type of seaweed species, wherein it occurred at 400nm for *E. intestinalis,* at 425 nm for *S. vulgare,* and at 448 nm for *A. taxiformis*. For AgNPs synthesized using cyanobacteria extracts, the UV-Vis absorption spectrum was measured every 30 min for *S. platensis,* where it exhibited longer time intervals of 24, 48, 72, and 96h. The SPR was recorded at 410 nm for *S. platensis* and at 451nm for *O. acuminate* (Fig. 1).

TABLE 1. The antibiotic test of the bacterial isolates susceptibility against diverse antibiotics

StandardAntibiotics[1]	Potency (µg/ disk)	Bacterial isolates[2]													
		S1	S2	S3	S4	S5	E1	E2	E3	E4	K1	K٢	P1	P2	Incidence of resistance percentage
S	15	R	R	R	S	R	I	R	R	R	R	R	R	R	92 %
AMC	30	R	R	S	S	R	R	R	S	R	S	R	R	S	61 %
MEM	30	R	R	R	S	R	R	S	I	R	R	R	R	S	70 %
OXA	10	R	R	R	R	R	R	R	R	S	R	R	R	S	85 %
AZ	15	R	R	R	R	S	R	R	S	R	R	S	S	S	62 %
FEB	30	I	R	R	R	R	R	R	R	R	R	S	R	I	85 %
CXM	30	R	S	R	R	R	R	R	R	R	R	R	R	R	92 %
CRO	30	R	I	R	R	R	R	R	R	S	R	S	I	R	85 %
SXT	30	R	R	R	S	R	R	R	R	S	R	R	R	R	85 %
LEV	10	R	R	R	I	R	R	R	R	R	R	R	R	S	92 %
AZM	15	R	R	R	R	R	R	R	R	R	R	R	R	R	100 %
CL	15	R	R	S	R	I	R	I	R	R	R	R	R	R	92 %
TE	30	R	R	S	R	R	R	S	R	R	I	S	R	R	77 %
Multiple antibiotics resistance index (MAR)		1.0	0.92	0.77	0.71	0.92	1.0	0.84	0.84	0.77	0.92	0.70	0.92	0.61	

R: Means Resistant, I: Means Intermediate, and S: Means Susceptible.[1]Antibiotic Standards: S= Streptomycin, AMC= Amoxicillin-clavulanic acid, MEM= Meropenem, OXA= Oxacillin, AZ= Aztreonam, FEB= Cefepime, CXM= Cefuroxime, CRO= Cefotriaxone, SXT=Trimethoprime-Sulfamethoxazole, LEV= Levofloxacin, AZM= Azithromycin, CL= Chloramphenicol, TE= Tetracycline. [2] Bacterial isolates: S = *S. aureus* isolates, S5= *S. epidermidis*, E= *E. coli* isolates, K= *K. pneumoniae* isolates, P= *P. aeruginosa* isolat

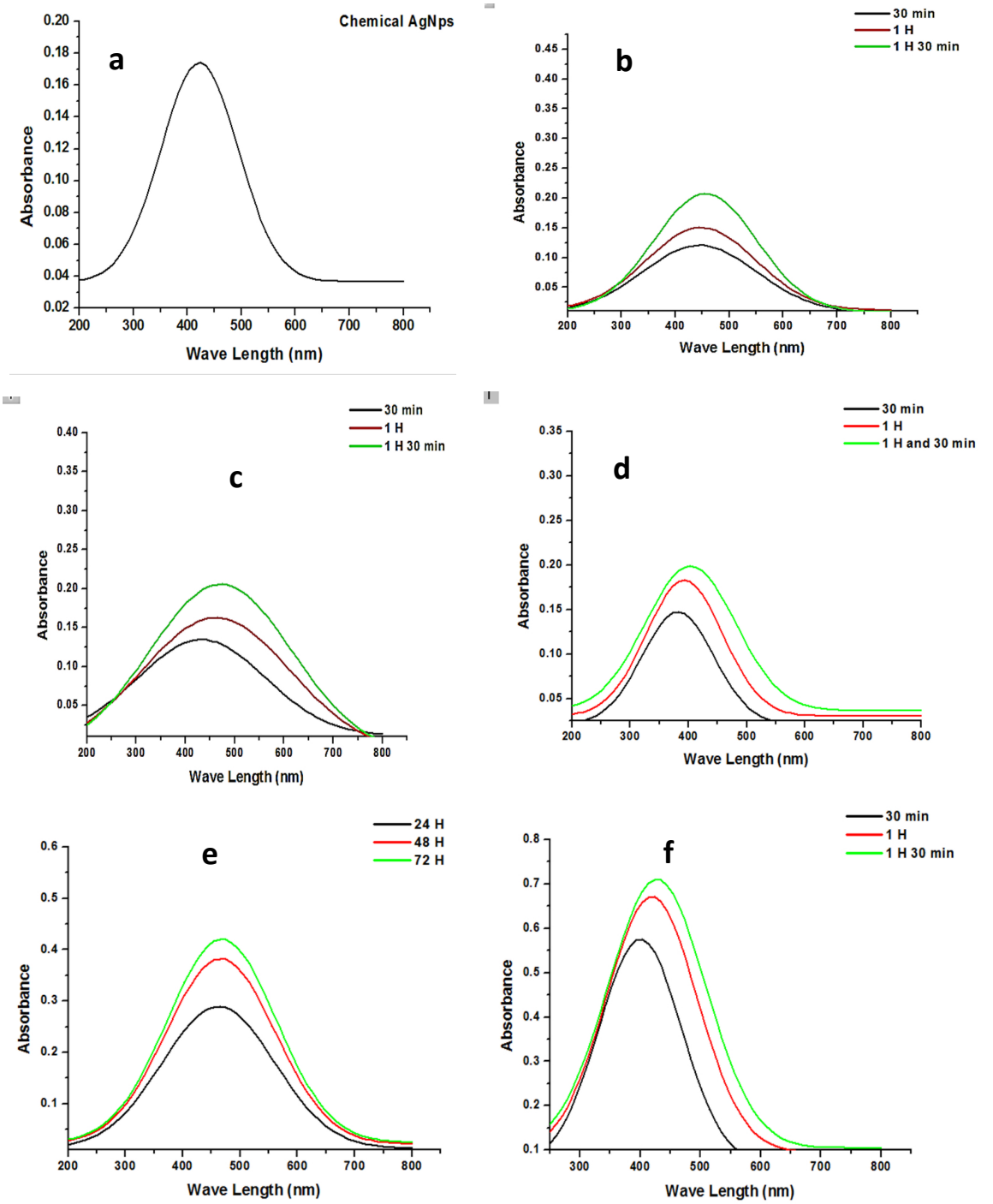

Fig. 1. UV-Vis spectrum of chemically (a) and biosynthesized AgNPs using *A. taxiformis* (b), *S. vulgare* (*c*), *S. platensis* (*d*), *O. acuminate* (e), and *E. intestinalis* (f)

Antibacterial activity of the chemically and biologically synthesized AgNPs

As revealed by the former results, all the examined algal biological extracts could successfully develop AgNPs. Therefore, the antibacterial activity test was performed for all the chemically and biosynthesized AgNPs to select the most effective AgNPs as antibacterial agent. As depicted in Table 2, the test was performed on the MDR pathogenic isolates of *S. aureus* (S1), *E. coli* (E1), *K. pneumoniae* (K1), *S. epidermidis* (S5), and *P. auroginosa* (P1). All the investigated AgNPs exhibited significant activity according to the target isolate susceptibility and the type

(source) of AgNPs. The maximum recorded inhibition zones were against S1 (38mm) and E1 (32mm) for *S. vulgare* (brown seaweed) extract derived AgNPs, followed by the chemically synthesized AgNPs, for which the inhibition zones were recorded at 39 and 35mm for S1 and E1, respectively, compared to the values obtained using the positive control antibiotic SXT. Similarly, AgNPs derived from *S. platensis* (cyanobacteria) showed inhibition zones at 30 and 26 mm for S1 and E1, respectively. Compared with SXT, S1 (G +ve) and E1 (G –ve) were the most sensitive bacterial isolates. Moreover, the chemically and biologically synthesized AgNPs (derived from *S. vulgare, S. platensis,* and *A. taxiformis* extracts, respectively) were promising antibacterial candidates. Therefore, further characterization of *S. vulgare* as well as the chemically synthesized AgNPs was conducted as following.

Characterization of the chemically and biologically synthesized AgNPs

FTIR analysis of the synthesized AgNPs

FTIR analysis was conducted to detect the functional groups in both the chemically and biologically synthesized (*S. vulgare*) AgNPs. Strong peaks observed at 3590 and 3583cm^{-1} were related to the O-H stretching of polysaccharides for both chemically and biosynthesized AgNPs, respectively. The peaks observed at 3431.71 and 3404.14cm^{-1} were assigned to NH stretch (amine), and those observed at 2377.82 and 2378.76cm^{-1} corresponded to O=C=O (carbonyl bond group) stretching. Peaks observed at 1639.21cm^{-1} for the chemically synthesized AgNPs and at 1638.23cm^{-1} for the biosynthesized AgNPs, represented the NH bend of amine and the stretching vibrations of –C=C– for proteins, amides and secondary amines or alkenes. Peaks observed at 1390.42 and 1383.68cm^{-1} were related to the C–H (alkanes) bend, and those observed at 1016.30 and 1102.12cm^{-1} indicated the presence of stretch vibration of C–O group (Table 3, Fig. 2).

TABLE 2. The antibacterial activity of chemically and biosynthesized AgNPs on different MDR bacterial isolates*

Bacterial isolate codes	Chemically synthesized AgNPs	Seaweed species			Cyanobacteria species		Sulfamethoxazole (SXT)
		E. intestinalis	*A. taxiformis*	*S. vulgare*	*S. platensis*	*O. acuminata*	
	Inhibition zone (mm)						
S1	39±0.05^{a}	29 ±0.01^{b}	28.5±0.04^{b}	38±0.00^{a}	30±0.05^{b}	10 ±0.7^{c}	25±0.05^{b}
S5	25±0.03^{a}	9±0.3^{c}	21±0.00^{b}	25±0.05^{a}	20 ±0.11^{b}	3 ±0.01^{d}	21±0.00^{b}
E1	35±0.05^{a}	20±0.02^{b}	27 ±0.1^{b}	32±0.05^{a}	26±0.06^{b}	15±0.00^{c}	18±0.05^{c}
K1	27±0.11^{a}	15 ±0.05^{c}	20±0.05^{b}	21±0.2^{b}	22±0.11^{b}	11±0.08^{c}	18±0.04^{b}
P1	21±0.100^{a}	12 ±0.00^{b}	18 ±0.02^{a}	12±0.12^{b}	18±0.03^{a}	12±0.00^{b}	14±0.1^{b}

Values are mean inhibition zone (mm) ± S.D of three replicates. Different letters in similar row indicating significant difference at $P \leq 0.05$.

TABLE 3. FTIR analysis of chemically and biosynthesized AgNPs showing functional groups

Band no.	Vibration mode (Functional group)	Compound types	Frequency cm^{-1}	
			Chem. AgNPs	Bio. AgNPs
1	O-H stretching	alcoholic or polysaccharide compounds	3590.1	3583.09
2	N–H stretch (amine)	primary amines and amides	3431.71	3404.14
3	O=C=O stretching	carbonyl bond group	2377.8	2378.76
4	N–H bend (amine)	stretching vibrations of –C=C– or C=O	1639.2	1638.23
5	C–H bend stretching or NO_2 stretch	Alkanes or Nitro Compounds	1390.42	1383.68
6	C–O	aliphatic amines	1016.3	1102.12
7	H-C-C-Br	alkyl bromide	642.179	673.035

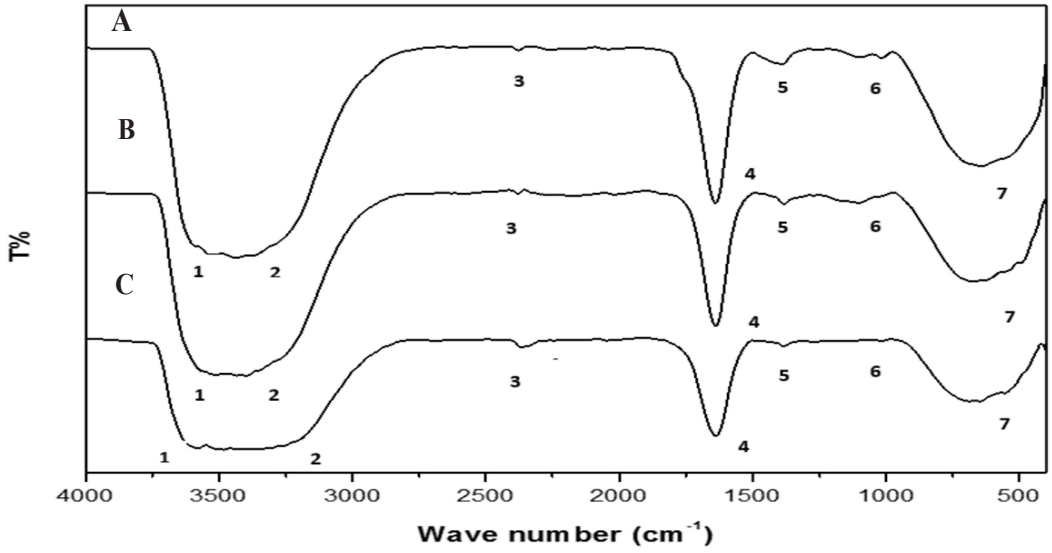

Fig. 2. FTIR analysis of the chemically (A), biosynthesized AgNPs (B) and the spectrum of the original *S. vulgare* extract (C)

XRD analysis of the synthesized AgNPs

The crystalline nature of nanoparticles was confirmed by XDR analysis and crystallography (Fig. 3). Four strong Bragg's reflection angles corresponding to silver °2θ plans at 38.36, 43.75, 64.8, and 77.6 were observed for the chemically synthesized AgNPs and at °2θ planes of 38.55, 44.3, 64.5, and 77.1 for the AgNPs biosynthesized from *S. vulgare* extract. These angles were consistent with the Ag+ ion crystal planes of 111, 200, 220, and 311, respectively. The average sizes of the chemically and biosynthesized nanoparticles, as calculated using Scherrer's equation, and were found to be 28.93 and 29.31nm, respectively, using the width of the 111 plane.

Zeta potential of the biosynthesized AgNPs

Zeta potential is a physical property that indicates the net surface charge of the NPs. The chemically and biologically synthesized AgNPs from *S. vulgare* extract showed a net charge of −50.3±10.4 and −52.1±10.8mV, respectively. The estimated conductivity values were 0.565 and 0.588mS/cm for chemically and biologically synthesized AgNPs, respectively. (Fig. 4). Therefore, as these values were within the documented Zeta potential range of greater than +30mV or less than −30mV, these AgNPs can be described as highly dispersed with good quality potential that enables significant degrees of particle stability.

TEM analysis of the biosynthesized AgNPs

TEM is a significant method to determine the morphology and average size of nanoparticles and their distribution in a colloidal solution (Fig. 5). The TEM results showed that AgNPs synthesized chemically or from *S. vulgare* filtrate were spherical in shape and well distributed with no aggregation. The mean particle size was 28.55nm for AgNPs synthesized by the chemical method and 29.02 nm for AgNPs synthesized by the biological method, which agreed with the previous XRD analysis results.

Cytotoxicity test of the synthesized AgNPs

The cytotoxic effect of the chemically synthesized and biosynthesized AgNPs was evaluated *in vitro* against human fibroblast normal cell lines at five serial concentrations for 24 and 48h (Fig. 6). After a 24h incubation at 1000mg/mL, the estimated cell viability for the chemically and biosynthesized AgNPs was 24.6% and 27.5%, respectively, and similar values were recorded at 48 h for both types of AgNPs. The concentration required to kill 50% of normal cells (IC_{50}) was 759.0µg/mL for the chemically synthesized AgNPs and 866.2µg/mL for the biosynthesized AgNPs at 24h, whereas it was 467.5 and 519.5µg/mL at 48h, respectively. This demonstrates the safety of biologically synthesized NPs. For the control AgNPs were replaced with sterilized distilled water. Therefore, the concentration of AgNPs at 100 µg/ml was chosen, as the safe concentration, for further experiments.

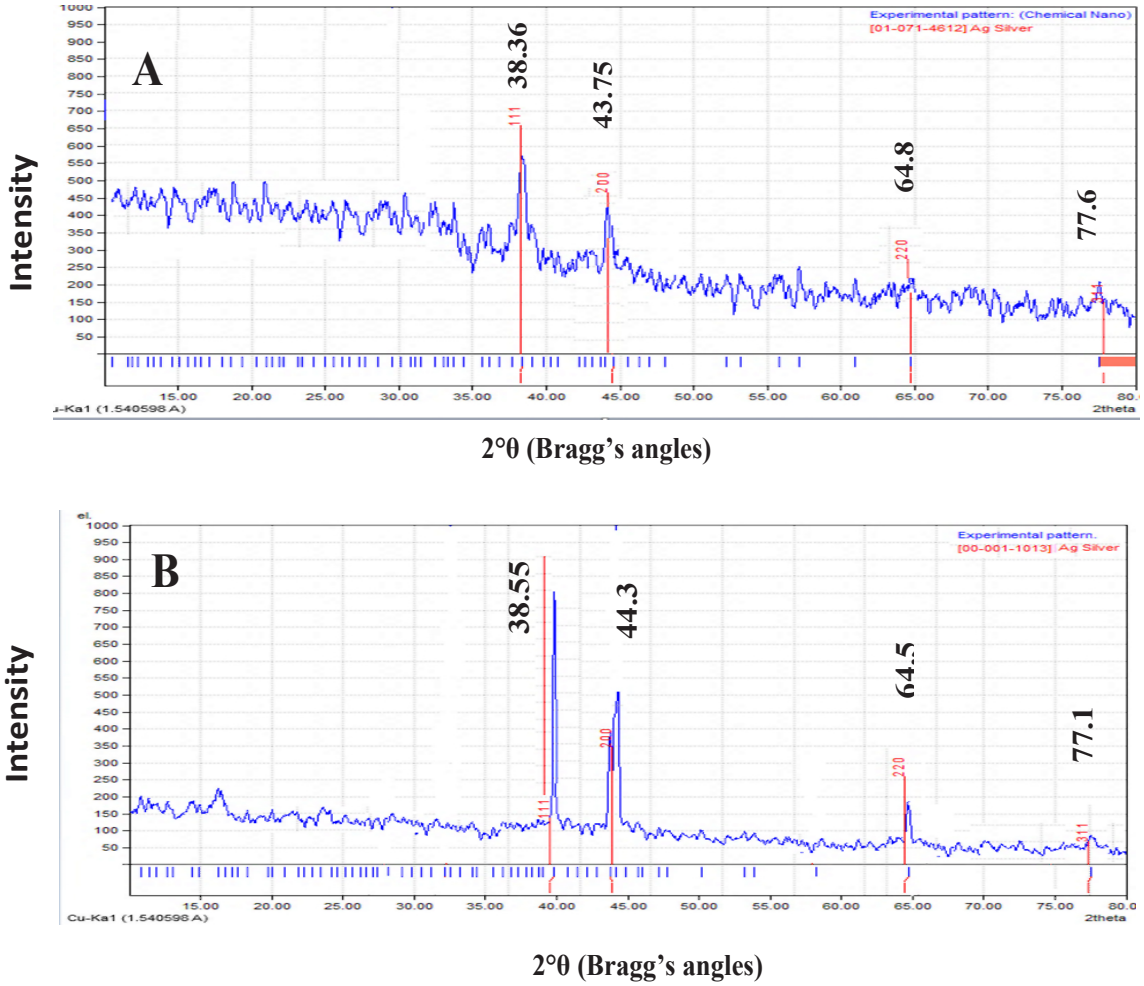

Fig. 3. XRD analysis of the chemically (A) and biosynthesized (B) AgNPs

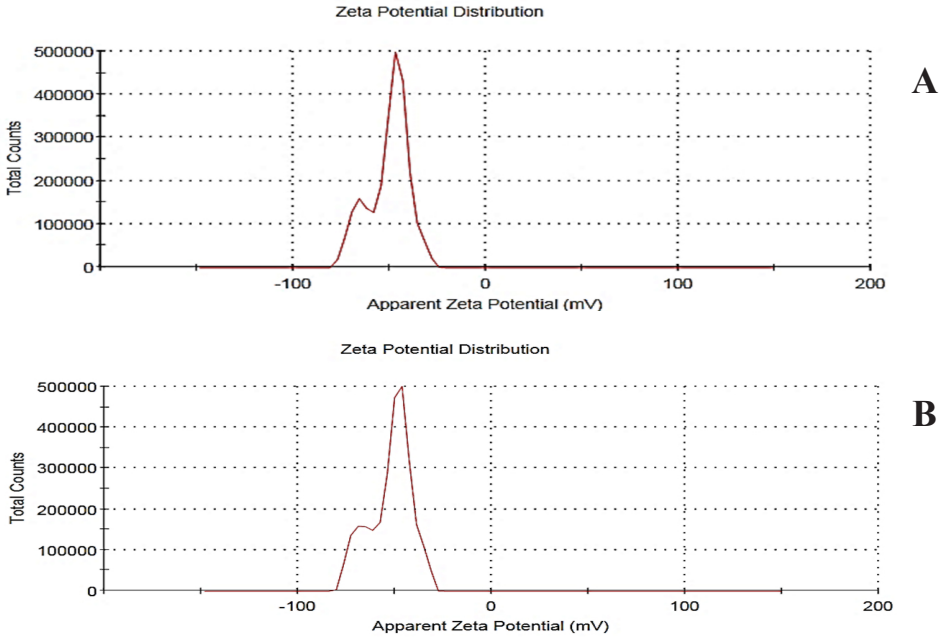

Fig. 4. Zeta potential analysis of the chemically (A) and biosynthesized (B) AgNPs

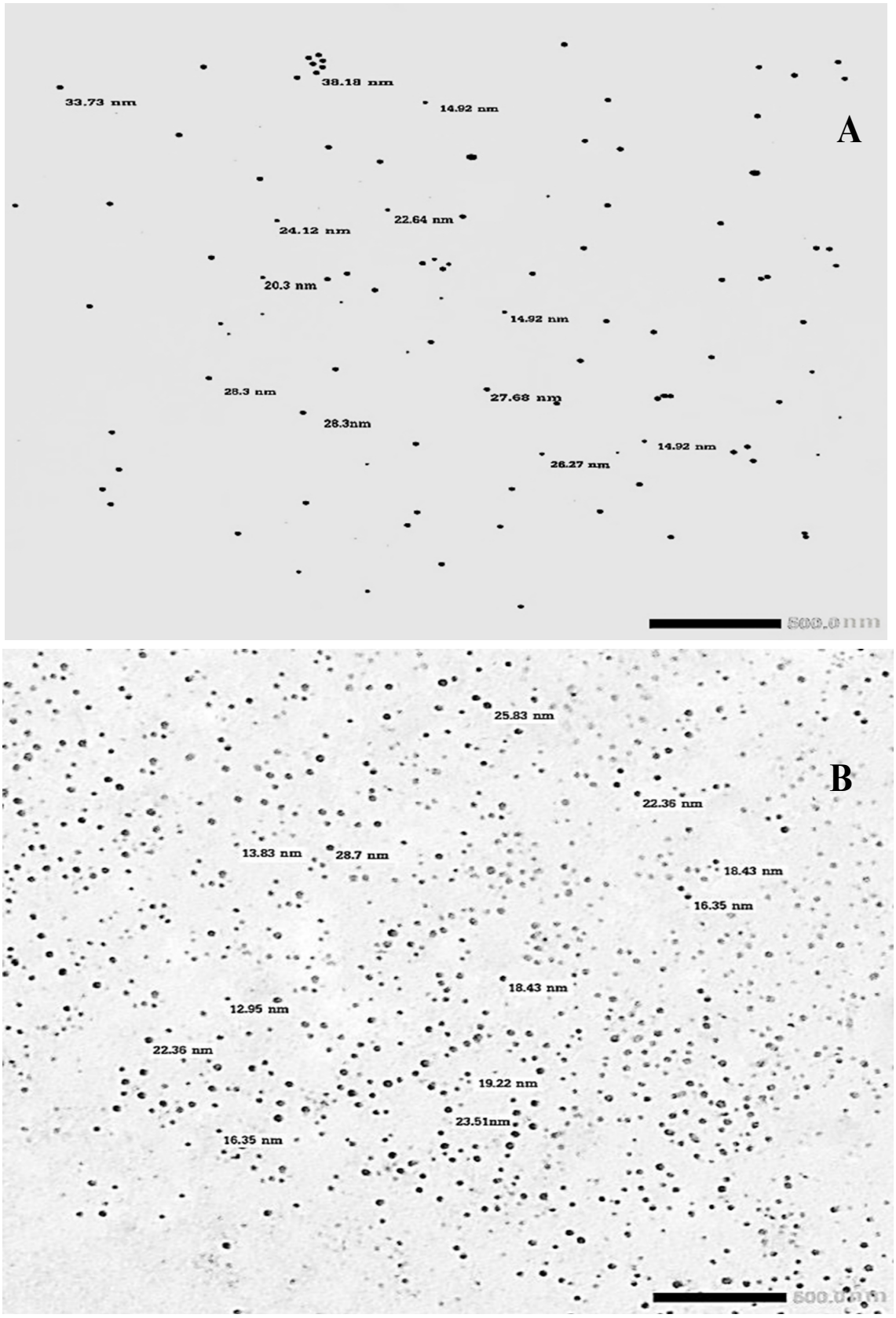

Fig. 5. TEM micrograph of the chemically (A) and biosynthesized (B) AgNPs (×500nm)

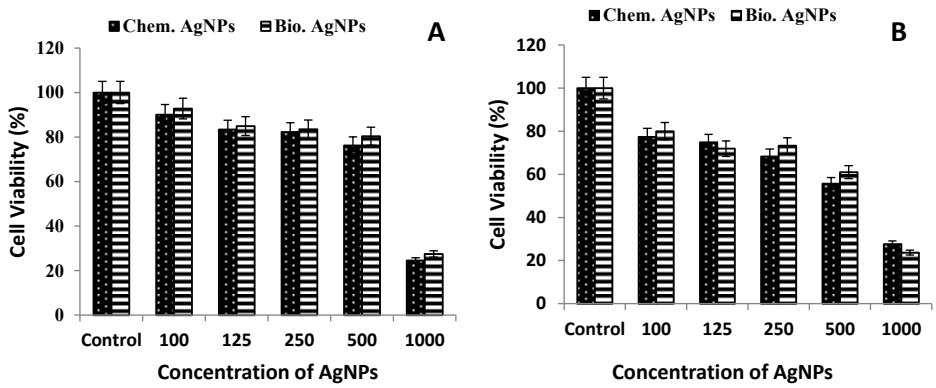

Fig. 6. Cytotoxicity test of chemically and biosynthesized AgNPs on normal cell line at 24h (A) and at 48h (B)

Production of silver loaded nanofilms with antibacterial activity for wound healing treatment

The AgNPs were loaded onto previously prepared PLA/PEG fiber films to make a silver-loaded nanofilms **(**PLA/PEG/AgNPs), and its antibacterial activity, *in vitro* was studied. According to the recorded results of the AgNPs susceptibility test, the two bacterial isolates *S. aureus* (S1) and *E. coli* (E1), were selected. Remarkably, these two strains are among the most common pathogens (Dermatophyte) that infect wounds and burns. The PLA/PEG film was loaded with a 100µg/mL concentration of AgNPs (which is the safe concentration that produced the maximum cell viability percentage according to the recorded results of the cytotoxicity test). Moreover, to ensure a safe effect on normal human tissues, the PLA/PEG/AgNPs nanofilms were incubated for 3 or 6 h to test against S1 and E1, *in vitro*. Results showed that control PLA/PEG fiber films (unloaded with AgNPs) demonstrated only 0.12: 0.15CFU/mL log reduction in the growth of both isolates. On the contrary, the effect of PLA/PEG/AgNPs nanofilms was found to be dependent on the incubation period, i.e., the longer the incubation period with bacteria, greater the growth inhibition. Furthermore, PLA/PEG/AgNPs exhibited greater antibacterial activity for the G+ve S1 isolate than for the G–ve E1 isolate. The log reduction in S1 growth was recorded at 2.4 and 2.8CFU/mL after 3 and 6h of incubation, respectively, in the case of PLA/PEG/bio-AgNPs. Lower values of 2.00 and 2.5CFU/mL were estimated after 3 and 6h, respectively, against E1 using the same bio-nanofilms. Similarly, the chemically synthesized AgNPs exhibited 2.3 and 3.00CFU/mL reductions in S1 growth after 3 and 6h of incubation, respectively, whereas they showed log reduction values of 1.54 and 2.73CFU/mL in E1 growth (Fig. 7).

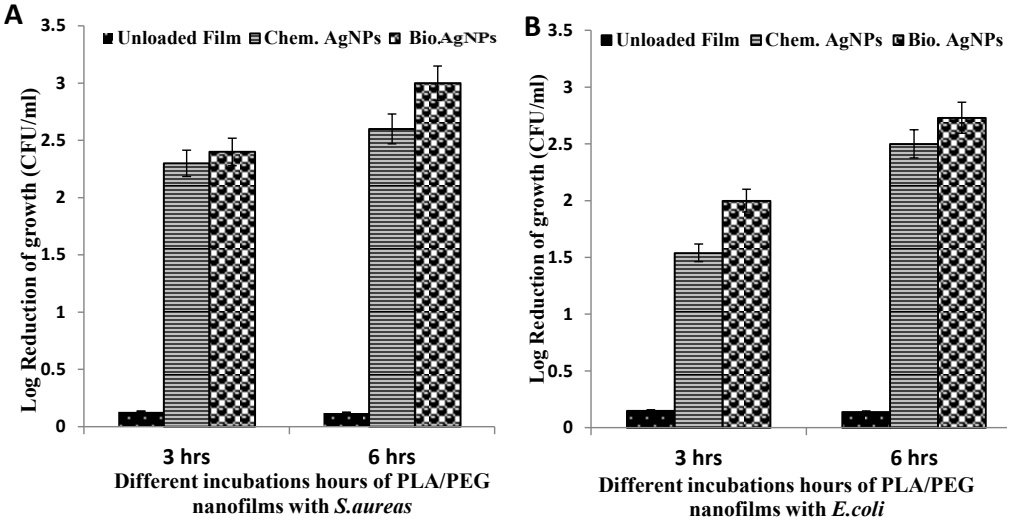

Fig. 7. The antibacterial activity of PLA/PEG/Ag nanofilms against A) *S. aureus* (S1) and B) *E. coli* (E1) after different incubation periods

Discussion

There exists an urgent need for novel antimicrobial agents. AgNPs are known to play an active role in the control of infection and wound healing along with their distinctive role in preventing infection and broad-spectrum antimicrobial efficacy (Paladini & Pollini, 2019).

In the present study, 13 G +ve and G –ve bacterial isolates were found to be resistant to two or more antibiotics of different classes, indicating MDR. These results were consistent with those reported by Garoy et al. (2021), who mentioned that all *S. aureus* isolates in their study were resistant to more than four tested antibiotics, including penicillin, vancomycin, clindamycin, and erythromycin. The bacterial isolates **S1** and **E1** were resistant to all the tested antibiotics in the present study as indicated by the MAR index values, followed by those for **K1** and **P1**. These findings concur with those observed by El-Shouny et al. (2017) who found that three isolates of *E. coli*, two isolates of *K. pneumoniae,* and three isolates of *P. mirabilis* had extreme MAR index value (> 0.2) with resistance estimation ranging from 63% to 100%, On the contrary, Parvin et al. (2021) reported that three isolates of *S. aureus* were broadly drug resistant and the maximum average of resistance was detected against cefoxitin, followed by oxacillin, amoxicillin-clavulanic acid, amoxicillin and cefixime.

In the present study, the AgNPs were synthesized by the chemical reduction method using TSC that acted as both reducing and coordinating agent (Syaiful et al., 2021). As a reductant, sodium acetate ($C_6H_5O_7Na_3$) reduced Ag^+ ions directly to produce metallic Ag^o atoms. Then, the generated Ag^o atoms acted as nucleation sites and catalyzed the reduction of residual metal ions found in the solution, turning it into a dark brown color (Yerragopu et al., 2020). The combination of atoms resulted in the development of metallic clusters, which were normally stabilized by surfactants, ligands and polymers using TSC that acted as a reducing co-agent (Ranoszek-Soliwoda et al., 2017). On the other hand, the biologically synthesized AgNPs from cyanobacteria or seaweed filtrates, were also visually confirmed by the color change from colorless to yellow, orange, violet, and finally reddish brown. Such a color transition is often indicative of changes in the metal oxidation state. Here, silver ion (Ag^+) was reduced by several biomolecules such as proteins, amino acids, and polysaccharides (which are commonly present in seaweeds and cyanobacteria extracts) into AgNPs. These results were consistent with those observed in several studies conducted using the green seaweed *E. compressa* (Ramkumar et al., 2017), and the brown seaweeds *Cystoseira crinite* (Elrefaey et al., 2022) and *S. wightii* (Ponmani et al., 2020). These results were also consistent with those of studies conducted using cyanobacteria such as *Leptolyngbya foveolarum* and *Anabaena flos-aquae* (Chugh et al., 2021), as well as *A. variabilis* and *S. platensis* (Ismail et al., 2021a).

The formation of AgNPs was further confirmed by sharp indicative peaks in the visible region of the UV-Vis spectrum. Both the chemically and biosynthesized AgNPs demonstrated characteristic peaks between 430 and 450 nm due to SPR of AgNPs formation. The SPR bands were relatively broad with an absorbance tail at longer wavelengths due to the size distribution of particles. The broadening of the peaks and the decrease in their in-between gaps indicate that particles are spherical and well dispersed (Bratovcic, 2020). The increase in the intensity of the peak is proportional to the increase in the concentration of the synthesized AgNPs in the measured solution. Hence, the biologically synthesized AgNPs from the different algal extracts were well comparable with the chemically synthesized AgNPs. Therefore, to determine the most active AgNPs as antibacterial agents, their activity was investigated against S1, S5, E1, K1 and P1 as the maximum MDR strains.

Results showed that, the chemically and biosynthesized AgNPs from *S. vulgare* had a notable antibacterial effect on both S1 (G +ve) and E1 (G –ve) strains. Deepak et al. (2018) found that AgNPs biosynthesized from *S. wightii* demonstrated antibacterial effects against *E. coli*, *P. aeruginosa*, *S. typhimurium*, *S. flexneri*, *B. subtilis*, *B. cereus* and *E. faecalis*. Similarly, López-Miranda et al. (2021) prepared AgNPs using filtrates from brown seaweed species *Sargassum natans* and *Sargassum fluitans*. They mentioned that the biosynthesized AgNPs were significantly more effective against *S. aureus* and *P. aeruginosa* than the chemically synthesized AgNPs using Polyvinylpyrrolidone (PVP) as a stabilizing agent. These results were also compatible with those reported by Skóra

et al. (2021) who investigated the antibacterial and antibiofilm activities of AgNPs against 18 medically important MDR bacteria including *S. aureus* and *E. coli*. They found that *Acinetobacter baumannii* and *S. aureus* strains, were the most affected.

Since the chemically and biosynthesized AgNPs from *S. vulgare* were the most effective antibacterial agents, their complete characterization was performed to fully determine the structural criteria that enabled their antibacterial capacity. According to the FTIR analysis results, several functional groups were identified in both synthesized AgNPs. The polysaccharide compounds may bind to silver ions, resulting in the formation of AgNPs (González-Fuentes et al., 2020). According to Azizi et al. (2013), the Van der Waals interaction among nitrogen and oxygen atoms in the biological compounds found in *Sargassum sp.* extracts are responsible for the synthesis and capping of AgNPs using a green method. The FTIR spectrum results support the existence of NH groups on the outer surface of the biosynthesized AgNPs, confirming that metabolically formed proteins may act as capping agents throughout the reduction of Ag particles and prevent agglomeration, thus allowing their robust stability (Theivasanthi & Alagar, 2013; Ismail et al., 2021b).

In this study, the crystalline shape of AgNPs was established by the XRD technique, wherein the results were consistent with those reported by Rezazadeh et al. (2020), who described that the presence of four intense peaks at (111), (200), (220), and (311) planes, respectively was congruent to the AgNPs and compatible with the Bragg's reflections of silver ions. The XRD pattern indicated that the synthesized AgNPs had a face centered cubic assembly and crystalline in shape which were consistent with the findings of El-Naggar et al. (2017) and Sayed Ahmed et al. (2021). The particle size of both AgNPs varied between 12 and 24nm. These values and shapes of the particles were relative to those estimated by TEM analysis, showing that the particles were sole spherical crystals. Accordingly, the antibacterial activity of the AgNPs depends on their diameter size (Dong et al., 2019), as it decreases by increasing the NPs size. These results were compatible with those of Dal Lago et al. (2011), who investigated the bactericidal activity of silver metallic particles against four different bacterial strains, viz., *E. coli, S. aureus, S. epidermidis,* and *Micrococcus lysodeikticus,* and found that smaller NPs (particle size radius of 8.5nm) exhibited higher bactericidal activity than larger NPs (11 nm). Furthermore, the zeta potential analysis indicated that nanoparticles of particles sizes >20 or <20 - mV have appropriate electrostatic repulsion forces to maintain stability in solution (Salehi et al., 2016), whereas a relatively high zeta potential suggests that the particles are highly scattered due to heavy repulsion forces between synthesized nanoparticles (Sikka et al., 2021). A negative Zeta potential of approximately −50.3 mV for the chemically synthesized AgNPs was recorded in the present study, suggesting their higher stability. The high negative potential (surface charge) value may be attributed to the effective functional constituents such as capping and stabilizer agents that are present in the citrate of TSC (Salvioni et al., 2017). A similar negative potential value was observed for the biologically synthesized AgNPs, which may be attributed to the effective functional constituents such as capping agents found in the extract solution of *S. vulgare.* Similarly, TEM is a direct and functional method to detect the morphology and particle shape of chemically and biosynthesized AgNPs, along with their dispersal symmetry (Dawadi et al., 2021). The TEM results of the chemically and biosynthesized AgNPs confirmed the development of spherical NPs, which are primarily spherical in shape through the production process (Khalil et al., 2021).

Considering the abovementioned characteristics of the investigated chemically synthesized and biosynthesized AgNPs, their antibacterial activity exhibited against MDR strains could be attributed to several mechanisms. When the silver ions liberated from AgNPs come in contact with bacterial cells, they might deactivate the synthesis of some proteins and enzymes essential for adenosine triphosphate (ATP) production or affect the bacterial DNA replication process (Agnihotri & Mukherji, 2014). Along with providing stability, bio-molecular capping with polysaccharides and proteins may provide binding ability to the NPs on the bacterial cell membranes, leading to their antibacterial property (Arun et al., 2017; Gheda et al., 2021). Currently, the most well-known antibacterial mechanism of AgNPs is interruption of the reaction of the respiratory chain by merging the sulfhydryl groups, causing oxidative damage

to DNA and proteins and lipid peroxidation, thus triggering cellular apoptosis (Hamed et al., 2017). AgNPs can also attach to the sulfur and phosphorous of DNA groups, which results in the destruction and aggregation of bacterial DNA by disrupting transcription and translation (Dasgupta et al., 2018).

Liao & Tjong (2019) reported the dosage, period, and size dependence of AgNPs cytotoxicity, for particles smaller than 10 nm in size. In the present study, the results demonstrated that the reduction in normal cell viability was directly proportional to the dose and incubation period of the AgNPs. Compatible with these results, Alsharif et al. (2020) reported that chemically and biosynthesized AgNPs exerted an efficient dose-dependent cytotoxic effect against normal Vero cell lines whose viable cell count decreased with increase in AgNPs concentration. Consistent with our study results, incubating human normal cell lines (WI 38) was affected by higher AgNPs concentrations (Salem et al., 2020; Algotiml et al., 2022). Based on the results of the *in-vitro* cytotoxicity and antibacterial activity, a safe dosage of 100mg/mL was selected for wound patches application to evaluate their antibacterial activity against S1 and E1 strains, the common dermatophyte pathogens found in wounds and burns.

A series of studies have integrated the antibacterial compound to PLA/PEG film polymers for numerous purposes (Swaroop & Shukla, 2018). AgNPs embedded with polymer coats are safe for normal cells and only perform as defensive transporters or enhancers for local anti-infective effects (Bakhsheshi et al., 2020). Wound healing is a complex process with several potential factors that may delay the healing process, including colonization by bacteria (Okur et al., 2020). MDR such as *K. pneumoniae, E. coli, P. aeruginosa*, *S. aureus,* and *S. epidermidis* are increasingly implicated in both acute and chronic wound infections (Bassetti et al., 2019). According to the results of this study, a high antibacterial activity towards S1 and E1 wound pathogenic bacteria has been estimated after 24h of treatment with chemically and biosynthesized PLA /PEG /AgNPs nanofilms. Similar results were reported by Turalija et al. (2016), who used PLA /PEG films to enhance the antibacterial property of chemically synthesized AgNPs, although they reported lower antibacterial efficiency against *S. aureus*. Moreover, the PLA/PEG films, which were free from the synthesized AgNPs, exerted no or a slight effect on the bacterial isolates as reported by Yang & Song (2016). Compared with the abovementioned results, the only advantage of this study is loading the biosynthesized AgNPs onto the PLA/PEG films to incorporate efficient antibacterial properties without cytotoxicity effects. Furthermore, according to the results of this study, these nanofilms can be designed as bandages, coverings or other types of wound dressings that can be easily changed at 3-6h intervals during biomedical applications to promote the wound healing process.

Conclusions

AgNPs play vital role in the advancement of nanoscience and nanotechnology. Due to their excellent antimicrobial properties, they have an excellent potential as wound healing material. In this study AgNPs were chemically and biologically synthesized using simple chemical compounds and biological extracts from cyanobacteria and seaweeds, respectively. UV-Vis spectroscopy confirmed the formation of AgNPs which was dependent on the incubation period. The synthesized AgNPs were stable in solutions form due to presence of natural capping agents such as proteins and polysaccharide groups present in the extracts. The AgNPs were also crystalline in nature, spherical in shape, and smaller in size with remarkable stability. Furthermore, the synthesized AgNPs were safe for the WI-38 human normal cell line after 24 h of incubation. The synthesized AgNPs exhibited maximum antibacterial activity against MDR isolates of *S. aureus* and *E. coli*. When the AgNPs were loaded onto PLA/PEG films, they led to a notable growth inhibition of *S. aureus* and *E. coli* after 3 and 6 h of incubation. Therefore, AgNPs can be efficiently synthesized from eco-friendly natural sources such as cyanobacteria and seaweeds. These biosynthesized AgNPs possess antibacterial properties against a wide array of MDR bacteria, including wound infecting pathogens. Hence, biosynthesized AgNPs can be used in pharmaceutical preparations or in biomedical applications to prevent nosocomial infections in the clinical environment.

Competing interests: The authors report no conflicts of interest regarding this work.

Authors' contributions: Project Supervision: Allam NG, Gaafar RM. Methodology and data analysis: Ismail GA, Attya P, El Zanaty M. Writing manuscript draft and editing: Ismail GA, Attya P, El-Zanaty M. All the authors contribute equally for conceptualization, writing final MS and approval.

Ethics approval: Not applicable.

References

Abdelmawgoud, Y., Abd El- Latif, W., Fawzy, N., Elnagdy, S. (2022). Prevalence of inducible clindamycin resistance and nanotechnological control of *Staphylococcus aureus* clinical isolates. *Egyptian Journal of Botany*, **62**(1), 73-84.

Agnihotri, S., Mukherji, S. (2014) Size-controlled silver nanoparticles synthesized over the range 5–100 nm using the same protocol and their antibacterial efficacy. *The Royal Society of Chemistry*, **4**, 3974–3983.

Aleem, A.A. (1993) "*The Marine Algae of Alexandria*", Egypt Univ. Alexandria, Alexandria, 139p.

Algotiml, R., Gab-Alla, A., Seoudi, R., Abulreesh, H.H., El-Readi, M.Z., Elbanna, K. (2022) Anticancer and antimicrobial activity of biosynthesized Red Sea marine algal silver nanoparticles. *Scientific Reports* **12**(1), 2421-35.

Alsharif, S.M., Salem, S.S., Abdel-Rahman, M.A., Fouda, A., Eid, A.M., El-Din, Hassan. S., Awad, M.A., Mohamed, A.A. (2020) Multifunctional properties of spherical silver nanoparticles fabricated by different microbial taxa. *Heliyon*, **6**, e03943- e03965.

Arun, S., Sonker, R., Jainendra, P., Rajneesh, V.K., Kannaujiya, R.P.S. (2017) Characterization and in vitro antitumor, antibacterial and antifungal activities of green synthesized silver nanoparticles using cell extract of *Nostoc sp*. strain HKAR-2. *Canadian Journal of Biotechnology*, **1**(1), 26-37.

Aslam, M., Fozia, F., Gul, A., Ahmad, I., Ullah, R., Bari, A., Mothana, R.A., Hussain, H. (2021). Phyto-extract-mediated synthesis of silver nanoparticles using aqueous extract of *sanvitalia procumbens*, and characterization, optimization and photocatalytic degradation of azo dyes orange g and direct blue-15. *Molecules*, **26**(20), 6144-6157.

Aswathy, A.S., Philip D. (2012) Green synthesis of gold nanoparticles using *Trigonella foenum-graecum* and its size-dependent catalytic activity. *Spectrochimica Acta Part A: Molecular Spectroscopy*, **97**, 1-5.

Azizi, S., Namvar, F., Mahdavi, M., Ahmad, M., Mohamad, R. (2013). Biosynthesis of silver nanoparticles using brown marine macroalga, *sargassum muticum* aqueous extract. *Materials*, **6**(12), 5942–5950.

Bakhsheshi-Rad, H.R., Ismail, A.F., Aziz, M., Akbari, M., Hadisi, Z., Khoshnava, S.M., Pagan, E., Chen, X. (2020) Co-incorporation of graphene oxide/ silver nanoparticle into Poly-L-lactic acid fibrous: A route toward the development of cytocompatible and antibacterial coating layer on magnesium implants. *Materials Science & Engineering. C, Materials for Biological Applications*, **111**, 110812-110828.

Ballotin, D., Fulaz, S., Souza, M.L., Corio, P., Rodrigues, A.G., Souza, A.O. (2016) Elucidating protein involvement in the stabilization of the biogenic silver nanoparticles. *Nanoscale Research Letters*, **11**(1), 313-322.

Bardania, H., Mahmoudi, R., Bagheri, H. (2020) Facile preparation of a novel biogenic silver-loaded Nanofilm with intrinsic anti-bacterial and oxidant scavenging activities for wound healing. *Scientific Reports,* **10**, 6129-6134.

Bassetti, M., Peghin, M., Vena, A., Giacobbe, D.R. (2019) Treatment of infections due to MDR gram-negative bacteria. *Frontiers in Medicine,* **6**, 74-84.

Bhuyar, P., Rahim, M.H.A., Sundararaju, S. (2020) Synthesis of silver nanoparticles using marine macroalgae *Padina* sp. and its antibacterial activity towards pathogenic bacteria. *Beni-Suef University Journal of Basic and Applied Sciences*, **9**, 3-18.

Bratovcic, A. (2020) Biosynthesis of green silver nanoparticles and its uv-vis characterization. *International Journal of Innovative Science, Engineering & Technology*, **7** (7), 170-176.

Chinnasamy, G., Chandrasekharan, S., Koh, TW., Bhatnagar, S. (2021) Synthesis, characterization, antibacterial and wound healing efficacy of silver nanoparticles from *Azadirachta indica*. *Frontiers in Microbiology*, **12**, 611560-611564.

Chugh, D., Viswamalya, V.S., Das, B. (2021) Green synthesis of silver nanoparticles with algae and the importance of capping agents in the process. *Journal, genetic engineering & biotechnology*, **19**(1), 126-147.

Chung, W.S., Walker, A.W., Louis, P., Parkhill, J., Vermeiren, J., Bosscher, D., Duncan, S.H., Flint, H.J. (2016) Modulation of the human gut microbiota by dietary fibres occurs at the species level. *BMC Biology*, **11**, 14-3.

CLSI (2021) "*Performance Standards for Antimicrobial Disk Susceptibility Tests; Approved Standard*", 11th ed.

Collee, J., Fraser, G., Marmion, P., Simmons, A. (1996) "*Practical Medical Microbiology*". 4th ed. Churchill, Livingstone, New York, pp. 413–418.

Dal Lago, V., Oliveira, L., Gonçalves, K., Kobarg, J., Cardoso, M. (2011) Size-selective silver nanoparticles: Future of biomedical devices with enhanced bactericidal properties. *Journal of Materials Chemistry,* **21**, 12267-12273.

Dasgupta, N., Ranjan, S., Mishra, D., Ramalingam, C. (2018) Thermal Co-reduction engineered silver nanoparticles induce oxidative cell damage in human colon cancer cells through inhibition of reduced glutathione and induction of mitochondria-involved apoptosis. *Chemico-Biological Interactions*, **295**, 109–118.

Dawadi, S., Katuwal, S., Gupta, A., Lamichhane, U., Thapa, R., Jaisi, S., Lamichhane, G., Bhattarai, D.P., Parajuli, N. (2021) Current research on silver nanoparticles: synthesis, characterization, and applications. *Journal of Nanomaterials Hindawi*, **2021**, 6687290-6687313.

Deepak, P., Amutha, V., Birundha, R., Sowmiya, R. (2018) Facile green synthesis of nanoparticles from brown seaweed *Sargassum wightii* and its biological application potential. *Advances in Natural Sciences: Nanoscience and Nanotechnology,* **9**(3), 035019-035029.

Dong, Y., Zhu, H., Shen, Y., Zhang, W., Zhang, Li. (2019) Antibacterial activity of silver nanoparticles of different particle size against *Vibrio Natriegens*. *PLoS ONE* ,**14**, e0222322-e222334.

El-Naggar, N., El-Ahmady, H., Mervat, H., El-Sawah, A.A. (2017) Bio-fabrication of silver nanoparticles by phycocyanin, characterization, in vitro anticancer activity against breast cancer cell line and *in vivo* cytotoxicity. *Scientific Reports*, **7**, 10844.

Elrefaey, A.A.K., El-Gamal, A. D., Hamed, S. M., El-belely, E.F., (2022) Algae-mediated biosynthesis of zinc oxide nanoparticles from Cystoseira crinite (Fucales; Sargassaceae) and it's antimicrobial and antioxidant activities. *Egyptian Journal of Chemistry*, **65**(4), 231-240.

El-Shouny, W.A., Gaafar, R.M., Ismail, G.A, El-zanaty, M.M. (2017) Antibacterial activity of some seaweed extracts against multidrug-resistant urinary tract bacteria and analysis of their virulence genes. *International Journal of Current Microbiology and Applied Sciences*, **6**(11), 2569-2586.

Fang, J., Zhang, C., Mu, R. (2005) The study of deposited silver particulate films by simple method for efficient SERS. *Chemical Physics Letters*, **401**, 271–275.

Garoy, E., Yohannes, G., Yacob, B., Achila, O., Okoth, T. (2021) Magnitude of multidrug resistance among bacterial isolates from surgical site infections in two national referral hospitals in Asmara, Eritrea. *International Journal of Microbiology*, **2021**, 6690222-6690233.

Gheda, S., Abo-Shady, A., Abdel-Karim, O., Ismail, G. (2021) Antioxidant and antihyperglycemic activity of *Arthrospira platensis* (spirulina platensis) methanolic extract: *In vitro* and *in vivo* study. *Egyptian Journal of Botany*, **61**(1), 71-93.

González-Fuentes, F.J., Molina, G.A., Silva, R., López-Miranda, J.L., Esparza, R., Hernandez-Martinez, A.R., Estevez, M. (2020) developing a cnt-spe sensing platform based on green synthesized AuNPs, using *Sargassum* sp. *Sensors*, **20**(21), 6108-6120.

Guiry, M.D., Guiry, G.M. (2019) Algae Base. World-wide electronic publication, National University of Ireland, Galway. http://www.algaebase.org; accessed on 4 December 2019.

Gupta, R.K., Kumar, V., Gundampati, R.K., Malviya, M., Hasan, S.H., Jagannadham, M.V. (2017) Biosynthesis of silver nanoparticles from the novel strain of *Streptomyces* Sp. BHUMBU-80 with highly efficient electroanalytical detection

of hydrogen peroxide and antibacterial activity. *Journal of Environmental Chemical Engineering*, **5**, 5624–5635.

Haider, M.J., Mehdi, M.S. (2014) Study of morphology and Zeta Potential analyzer for the Silver Nanoparticles. *International Journal of Scientific & Engineering Research*, **5**(7), 381- 387.

Hamed, S., Emara, M., Shawky, R.M., El-Domany, R.A., Youssef T. (2017) Silver nanoparticles: antimicrobial activity, cytotoxicity, and synergism with N-acetyl cysteine. *Journal of Basic Microbiology,* **57**(8), 659–668.

Hassan, M., Le Guen, M.J., Tucker, N., Parker, K. (2019) Thermo-mechanical, morphological and water absorption properties of thermoplastic starch/ cellulose composite foams reinforced with PLA. *Cellulose,* **26**(7), 4463-4478

Ismail, G.A., El-Sheekh, M.M., Samy, R.M., Gheda, S.F. (2021a) Antimicrobial, antioxidant, and antiviral activities of biosynthesized silver nanoparticles by phycobiliprotein crude extract of the cyanobacteria *Spirulina platensis* and *Nostoc linckia*. *BioNanoScience*, **11**(4). DOI:10.1007/ s12668-021-00828-3

Ismail, G.A., Allam, N.G., El-Gemizy, W.M., Salem, M.A. (2021b) The role of silver nanoparticles biosynthesized by *Anabaena variabilis* and *Spirulina platensis* cyanobacteria for malachite green removal from wastewater. *Environmental Technology*, **42**(28), 4475-4489.

Khalil, M.A., El Maghraby, G.M., Sonbol, F.I., Allam, N.G., Ateya, P.S., Ali, S.S. (2021) Enhanced efficacy of some antibiotics in presence of silver nanoparticles against multidrug resistant *pseudomonas aeruginosa* recovered from burn wound infections. *Frontiers in Microbiology,* **12**, 2645-2665.

Khan, I., Saeed, K., Khan, I. (2019) Nanoparticles: properties, applications and toxicities. *Arabian Journal of Chemistry*, **12**(7), 908-931

Kirby-Bauer, W.M.M., Bauer, A.W., Sherris, J.C., Turck, M. (1966) Antibiotic susceptibility testing by a standardized single disk method. *American Journal of Clinical Pathology*, **45**(4), 493–496

Krishnan, P.D., Banas, D., Durai, R.D., Kabanov, D., Hosnedlova, B., Kepinska, M., Fernandez, C., Ruttkay-Nedecky, B., Nguyen, H.V., Farid, A., Sochor, J., Narayanan, V., Kizek, R. (2020) Silver nanomaterials for wound dressing applications. *Pharmaceutics*, **12**(9), 821-845.

Lee, N.Y., Ko, W.C., Hsueh, P.R. (2019) Nanoparticles in the treatment of infections caused by multidrug-resistant organisms. *Frontiers in pharmacology*, **10**, 1153-1163.

Liao, C., Li, Y., Tjong, S.C. (2019) Bactericidal and cytotoxic properties of silver nanoparticles. *International Journal of Molecular Sciences*, **20**, 449-496.

Loo, Y.Y., Rukayadil, Y., Nor-Khaizura, M.A.R., Kuan, C.H., Chieng, B.W., Nishibuchi, M. (2018) *In vitro* antimicrobial activity of green synthesized silver nanoparticles against selected gram-negative foodborne pathogens. *Frontiers in Microbiology*, **9**, 1555-1562.

López-Miranda, J.L., Esparza, R., González-Reyna, M.A., España-Sánchez, B.L., HernandezMartinez, A.R., Silva, R., Estévez, M. (2021) *Sargassum* influx on the Mexican Coast: A source for synthesizing silver nanoparticles with catalytic and antibacterial properties. *Applied Sciences,* **11**(10), 4638-4649.

Magiorakos, A.P., Srinivasan, A., Carey, R.B., Carmeli, Y., Falagas, M.E., Giske, C.G., Harbarth, S., Hinndler J.F. (2014**)** Multidrug-resistant, extensively drug-resistant and pandrug-resistant bacteria. *Clinical Microbiology and Infection*, **8**(3), 268–281.

Mahmoudi, R., Ardakani1Maryam, T., Verdom, B.H., Bagheri, A., Beigi, M.H. (2019) Chitosan nanoparticles containing Physalis alkekengi-L extract: preparation, optimization and their antioxidant activity. *Bulletin of Materials Science*, **42**(3), 131-137.

Mehta, B., Chhajlani, M., Shrivastava, B. (2017) Green synthesis of silver nanoparticles and their characterization by XRD. *Journal of Physics: Conference Series*, **836**, 012024-50.

Menaa, F., Wijesinghe, U., Thiripuranathar, G., Althobaiti, N.A., Albalawi, A.E., Khan, B.A., Menaa, B. (2021) Marine algae-derived bioactive compounds: A new wave of nanodrugs? *Marine*

Drugs, **19**(9), 484-520.

Nqakala, Z.B., Sibuyi, N.R.S., Fadaka, A.O., Meyer, M., Onani, M.O., Madiehe, A.M. (2021) Advances in nanotechnology towards development of silver nanoparticle-based wound-healing agents. *International Journal of Molecular Sciences*, **22**(20), 11272-98.

Okur, M., Evren, K.I.D., Şenyiğit, Z., Üstündağ, O.N., Siafaka, P.I. (2020) Recent trends on wound management: New therapeutic choices based on polymeric carriers. *Asian Journal of Pharmaceutical Sciences*, **15**(6), 661-684.

Othman, L., Sleiman, A., Abdel-Massih, R.M. (2019) Antimicrobial activity of polyphenols and alkaloids in middle eastern plants. *Frontiers in Microbiology*, **10**, 911-939.

Oxoid (1981) "*The Oxoid Manual of Culture Media Ingredients and Other Laboratory Servies*". 5th ed. Oxoid, Manual, UK.

Paladini, F., Pollini, M. (2019) Antimicrobial silver nanoparticles for wound healing application. progress and future trends. *Materials (Basel, Switzerland),* **12**(16), 2540-2556.

Parvin, M.S., Ali, M.Y., Talukder, S., Nahar, A., Chowdhury, E.H., Rahman, M.T., Islam, M.T. (2021) Prevalence and multidrug resistance pattern of methicillin resistant *S. aureus* isolated from frozen chicken meat in Bangladesh. *Microorganisms*, **9**, 636-652.

Paul, J.P., Yadav, R.P. (2014) Green chemistry: An approach for synthesis of silver nanoparticles and their antimicrobial activity. *American Journal of Pharm Tech Research*, **4**(3), 489-498.

Ponmani, J., Kanakarajan, S., Selvaraj, R., Kamalanathan, A. (2020) Antioxidant properties of green synthesized silver nanoparticles from *Sargassum wightii. Saudi Journal of Medical and Pharmaceutical Sciences,* **6**(8), 516-525.

Rajeshkumar, S., Malarkodi, C., Paulkumar, K., Vanaja, M., Gnanajobitha, G., Annadurai, G. (2014) Algae mediated green fabrication of silver nanoparticles and examination of its antifungal activity against clinical pathogens. *International Journal of Metals*, 1-8. https://doi.org/10.1155/2014/692643

Ramkumar, V.S., Pugazhendhi, A., Gopalakrishnan, K., Sivagurunathan, P., Saratale, G.D., Dung, T., Kannapiran, E. (2017) Biofabrication and characterization of silver nanoparticles using aqueous extract of seaweed *Enteromorpha compressa* and its biomedical properties. *Biotechnology reports (Amsterdam, Netherlands)*, **14**, 1–7.

Ranoszek-Soliwoda, K., Tomaszewska, E., Socha, E., Krzyczmonik, P., Ignaczak, A., Orlowski, P., Krzyzowska, M., Celichowski, G., Grobelny, J. (2017) The role of tannic acid and sodium citrate in the synthesis of silver nanoparticles. *Journal of Nanoparticle Research: An Interdisciplinary Forum for Nanoscale Science and Technology*, **19**(8), 273-288.

Rezazadeh, N.H., Buazar, F., Matroodi, S. (2020) Synergistic effects of combinatorial chitosan and polyphenol biomolecules on enhanced antibacterial activity of biofunctionalized silver nanoparticles. *Scientific Reports*, **10**, 19615-19629.

Rippka, R., Deruelles, J., Waterbury, J.B., Herdman, M., Stanier, R. (1979) Generic assignments, strain histories and properties of pure cultures of cyanobacteria. *Journal of General Microbiology*, **111**, 1–61.

Salehi, S., Ataollah, S., Shandiz, S., Ghanbar, F., Darvish, M.R., Ardestani, M.S., Mirzaie, A., Jafari, M. (2016) Phytosynthesis of silver nanoparticles using *Artemisia marschalliana* Sprengel aerial part extract and assessment of their antioxidant, anticancer, and antibacterial properties. *International Journal of Nanomedicine*, **11**, 1835–1846.

Salem, S.S., Fouda, M.M.G., Fouda, A., Awad, M.A., Al-Olayan, E.M., Allam, A.A., Shaheen, T.I. (2020) Antibacterial, cytotoxicity and larvicidal activity of green synthesized selenium nanoparticles using *Penicillium corylophilum*. *Journal of Cluster Science*, **32**, 351-361.

Salvioni, L., Galbiati, E., Collico, V., Alessio, G., Avvakumova, S., Corsi, F., Tortora, P., Prosperi, D., Colombo, M. (2017) Negatively charged silver nanoparticles with potent antibacterial activity and reduced toxicity for pharmaceutical preparations. *International Journal of Nanomedicine*, **12**, 2517-2530.

Samuel, M.S., Jose, S., Selvarajan, E., Mathimani, T., Pugazhendhi, A. (2020) Biosynthesized silver nanoparticles using Bacillus amyloliquefaciens application for cytotoxicity effect on A549 cell line and photocatalytic degradation of p-nitrophenol. *Journal of Photochemistry & Photobiology, B: Biology*, **202**, 111642-52.

Saranya devi, J.S.K., Sruthy, P.B., Anjana, J.C., Rathinamala, J. (2014) Study on antibacterial activity of natural dye from the bark of *Araucaria columnaris* and its application in textile cotton fabrics. *Journal of Microbiology and Biotechnology,* **4**(3), 32-35.

Sayed Ahmed, H.I., Elsherif, D.E., El-Shanshory, A.R., Haider, A.S., Gaafar, M.R. (2021) Silver nanoparticles and *Chlorella* treatments induced glucosinolates and kaempferol key biosynthetic genes in *Eruca sativa*. *Beni-Suef University Journal of Basic and Applied Sciences*, **10**(1), 52-67.

Sikka, A., Sodimalla, T., Nagaraju, Y. (2021) Biosynthesis of silver nanoparticles and their biocontrol potentials against *Aspergillus Niger* and *Fusarium Udum*. *Research Square*, **10**(21203).

Skóra, B., Krajewska, U., Nowak, A. (2021) Non-cytotoxic silver nanoparticles as a new antimicrobial strategy. *Scientifc Reports*, **11**, 13451-65.

Stan, D., Enciu, A., Mateescu, A.L., Ion, A.C., Brezeanu, A.C., Stan, D., Tanase, C. (2021) Natural compounds with antimicrobial and antiviral effect and nanocarriers used for their transportation. *Frontiers in Pharmacology*, **12**, 2405-30.

Suriya, J., Bharathi, R.S., Sekar, V., Rajasekaran, R. (2012) Biosynthesis of silver nanoparticles and its antibacterial activity using seaweed *Urospora* sp. *African Journal of Biotechnology*, **11**(58), 12192–12198.

Swaroop, C., Shukla, M. (2018) Mechanical optical and antibacterial properties of polylactic acid/ polyethylene glycol films reinforced with MgO Nanoparticles. *Materials Today: Proceedings,* **5**, 20711–20718.

Syaiful, A.M., Ulfiya, E., Sentosa, P.A. (2021) Synthesis silver nanoparticles using trisodium citrate and development in analysis method. *AIP Conference Proceedings*, **2360**(1), 050007-17.

Theivasanthi, T., Alagar, M.K. (2013) Biomolecules assisted–rod/spherical shaped lead Nano powder synthesized by electrolytic process and its characterization studies. *Nano Biomedicine and Engineering*, **5**, 11–19.

Turalija, M., Bischof, S., Budimir, A., Gaan, S. (2016) Antimicrobial PLA films from environment friendly additives. *Composites Part B: Engineering*, **102**, 94–99.

Vasquez, Y., Hand, W. (2004) Antibiotic susceptibility patterns of community- acquired urinary tract infection isolates from female patients on the US (Texas)-Mexico border. *Journal of Applied Research*, **4**, 321-326.

Wang, Y., Herron, N. (1991) Nanometer-sized semiconductor clusters. materials synthesis, quantum size effects, and photophysical properties. *The Journal of Physical Chemistry*, **95**, 525–532.

Yang, H.J., Song, K.B. (2016) Application of lemongrass oil-containing polylactic acid films to the packaging of pork sausages. *Korean Journal for Food Science of Animal Resources*, **36**(3), 421-426.

Yerragopu, P.S., Hiregoudar, S., Nidoni, U., Ramappa, K.T., Sreenivas, A., Doddagoudar, S. (2020) Chemical synthesis of silver nanoparticles using tri-sodium citrate, stability study and their characterization. *International Research Journal of Pure and Applied Chemistry*, **21**, 37-50.

Zarrouk, C. (1966) Contribution à l'étude d'une cyanophycée. Influence de divers' facteurs physiques et chimiques sur la croissance et la photosynthèse de *Spirulina maxima*. (Setch et Gardner) Geitler. *Ph.D. Thesis*, Université de Paris, Paris, France.

Zawrah, M., Abd El-Moez, S. (2011) Antimicrobial activities of gold nanoparticles against major foodborne pathogens. *Life Science Journal*, **8**(4), 37-44.

Zazo, H., Colino, C.I., Lanao, J.M. (2016) Current applications of nanoparticles in infectious diseases. *Control Release*, **224**, 86–102.

Zhang, D., Ma, X., Gu, Y., Huang, H., Zhang, G. (2020) Green synthesis of metallic nanoparticles and their potential applications to treat cancer. *Frontiers in Chemistry*, **8**, 799-817.

تأثير جزيئات الفضة النانوية المخلقة كيميائيا وبيولوجيا على العزلات البكتيرية متعددة المقاومة للمضادات الحيوية والمسببة للأمراض الجلدية

جيهان احمد اسماعيل، نانيس جمال الدين علام، رضا محمد جعفر، مروة محمد البسيونى الزناتى، بريهان صالح عطية

قسم النبات- كلية العلوم – جامعة طنطا- طنطا- مصر.

فى الدراسة الحالية تم تخليق جزيئات الفضة النانوية باستخدام طرق كيميائية وبيولوجية. تم استخدام ثلاثى سيترات الصوديوم كعامل اختزال وتثبيت للتخليق الكيميائي. وللتخليق البيولوجي تم استخدام مستخلص من ثلاث طحالب بحرية وهي: انتيرومورفا وسارجاسوم واسبراجوبسيس. كما تم استخدم رشيح نوعين من البكتريا الخضراء المزرقة وهما: سبيرولينا واوسيلاتوريا. وقد تم التحقق من تكويين جزيئات الفضة النانوية بأستخدام التحليل الطيفي المرئي فوق البنفسجي. ثم تم تاكيده بواسطة عدة تحاليل كيميائية وهى الأشعة السينية، طيف الأشعة تحت الحمراء والمجهر الإلكتروني النافذ. وقد أظهرت نتائج تحليل الاشعة السينية الطبيعة البلورية لجزيئات الفضة النانوية المنتجة بمتوسط حجم 28.93 و29.31 نانوميتر لجزيئات الفضة النانونية المصنعة كيميائيا وبيولوجيا على الترتيب. وسجل تحليل جهد الزيتا 10.4±50.3- mV و 10.8± 52.1- Vm لكلا النوعين من جزيئات الفضة النانوية على الترتيب. وقد اظهرت جزيئات الفضة النانوية التى تم تخليقها سواء كيميائيا أو بيولوجيا تأثيرا بارزا على العزلات البكتيرية متعددة المقاومة للمضادات الحيوية وهى: استافيلوكوكس اوريس، اشيريشيا كولاى، كليبسيلا نيومونياي، سيديموناس ايروجينوزا واستافيلوكوكس ابيديرميدس بالمقارنة بالسلفاميثوكسازول كمضاد حيوى قياسي حيث اظهرت جزيئات الفضة النانوية المصنعة بيولوجيا اعلى نشاط ضد بكتيرى. وكذلك أثبت تحليل السمية أن جزيئات الفضة النانوية المخلقة كانت آمنة على الخلايا الليفية الطبيعية بجسم الانسان لمدة 24 ساعة. بالاضافة على ذلك فقد تم تحميل جزيئات الفضة النانوية المصنعة كيميائيا أو بيولوجيا على طبقات رقيقة من البولي لاكتيك اسيد/ والبولي ايثيلين جليكول(PLA/PEG) والتى اظهرت كفاءة ضد بكتيرية واعدة على العزلات البكتيرية المسببة لعدوى الجروح بعد 3 و 6 ساعات من المعالجة بهذة الاغشية المحملة بجزيئات الفضة النانوية. ولذلك توصي الدراسة الحالية باستخدام جزيئات الفضة النانوية المصنعة من مصادر طحلبية بيولوجية على وجه الخصوص فى علاج عدوى الجروح و التطبيقات العلاجية كبديل آمن واقتصادي عن المعاملات العلاجية الكيميائية.